Available online at http://scik.org
Commun. Math. Biol. Neurosci. 2026, 2026:10
https://doi.org/10.28919/cmbn/9734
ISSN: 2052-2541

MODELING THE IMPACT OF PUBLIC OPINION AND PREVENTIVE PRACTICES ON MALARIA TRANSMISSION IN CENTRAL AND NORTHERN BENIN

KASSIFOU TRAORE*, AUREL B. FRIDOLIN HANSINON, ROMAIN GLÈLÈ KAKAÏ

Laboratoire de Biomathématiques et d'Estimations Forestières, University of Abomey-Calavi, Cotonou, Bénin

Abstract. Malaria remains a major public health challenge in Sub-Saharan Africa, especially in Northern Benin, where seasonal variations drive transmission. The success of prevention and treatment depends on community compliance, which is influenced by public risk perception and social attitudes. Despite the widespread implementation of preventive interventions, malaria transmission persists at alarming levels in many regions. Existing mathematical models have often overlooked the role of population opinions and behavioral responses in shaping the effectiveness of these interventions. To address this gap, we extended a mathematical model integrating malaria transmission dynamics with an opinion dynamics framework. The study was conducted across four Benin districts, using five years (2019–2023) of real-world malaria surveillance data from the National Malaria Control Program. Behavioral data were derived from the 2022 Malaria Behavior Survey. The model was calibrated using nonlinear least squares estimation techniques. Analytical results confirm the positivity and boundedness of the model, and a disease-free periodic solution was established. The control reproduction number (R_c) was computed using the monodromy matrix method. The numerical analysis revealed that increased the percentage of favorable adherence to prophylactic measures results in a slight but consistent decrease in malaria incidence. Specifically, in Bantè, when partial adherence rose from 52% to 100%, the effective reproduction number decreased by 82.75%. Furthermore, we also note that a higher baseline influence rate (Ω_0) contributed to a substantial reduction in effective reproduction number. In Sinendé, increasing Ω_0 from 0.05 to 50 reduced malaria incidence by 17.65%.

*Corresponding author
E-mail address: traorekassifou45@gmail.com
Received December 07, 2025

The findings highlight that incorporating population behaviors and opinions into disease modeling enhances the effectiveness of public health strategies for sustainable malaria control in endemic areas.

Keywords: seasonality; malaria transmission; preventive measures; opinion dynamics; control reproduction number.

2020 AMS Subject Classification: 92D30.

1. INTRODUCTION

Malaria is an ancient disease that continues to cause harm to humans. It remains a major public health issue in low and middle-income countries, with control and elimination being top priorities in areas where it is widespread. This disease poses significant health and socio-economic challenges, affecting an estimated 3.2 billion people worldwide who are at risk of infection [1]. Despite the interventions implemented to control this disease, malaria continues to harm humanity. According to the World Health Organization (WHO), an estimated 249 million malaria cases and about 608,000 deaths occurred globally in 2022, representing a slight increase compared with 2021. The WHO African Region remains the most affected, accounting for around 94% of global cases and 95% of deaths. Despite this high burden, mortality among children under five has declined substantially over the past two decades, from more than 90% of malaria deaths in 2000 to about 78% in 2022 [1]. Since 2000, the Roll Back Malaria campaign has significantly enhanced intervention coverage and the expansion of effective treatments across Sub-Saharan Africa, achieving unprecedented levels of success [2]. The Global Technical Strategy for Malaria 2016–2030 (GTS) the World Health Organization (WHO) has established new objectives, targeting a reduction in global malaria incidence and mortality rates by at least 90%, and aiming for the elimination of the disease in at least ten countries by 2020, 20 countries by 2025, and 30 countries by 2030 [3].

Malaria is a communicable disease primarily found in tropical and subtropical regions, caused by the *Plasmodium* protozoan parasites [4]. The disease is transmitted to humans through the bite of infected mosquitoes. When such a mosquito bites a healthy individual, it transmits the *Plasmodium* parasite. To control vector-borne diseases like malaria represents a significant global public health challenge in the twenty-first century [4]. Vector control is a

crucial element in the efforts to control and eliminate malaria. The ability of vectors to transmit parasites and their susceptibility to control measures differ among mosquito species and are affected by local environmental conditions. Several measures are implemented to prevent malaria, including the use of insecticide-treated nets (ITNs) and indoor residual spraying (IRS). Insecticide-treated nets (ITNs) are categorized into two types: long-lasting insecticidal nets (LLINs), which have insecticide embedded into the fibers during manufacturing for extended effectiveness and standard insecticide-treated nets (ITNs), which require re-impregnation with insecticides every six months [5]. Indoor residual spraying (IRS) involves applying insecticides to the interior walls of homes to kill mosquitoes that come into contact with these surfaces [5]. Among these measures, insecticide-treated nets (ITNs) appear to be the most effective preventive measure against malaria transmission [5]. The use of long-lasting insecticide-treated nets and indoor residual spraying has helped reduce the burden of malaria in sub-Saharan Africa [4].

Mathematical models have been crucial in clarifying disease transmission dynamics, simplifying complex biological information, and enabling predictions for lesser-known scenarios. Epidemiologists extensively use these models to forecast malaria epidemics and guide eradication strategies [6, 7]. Combining multiple modeling approaches, rather than relying on a single model, is believed to improve long-term malaria control and elimination efforts [7].

Beyond biological and climatic factors, human behavior and public opinion profoundly influence malaria control outcomes. Thus, in addition to account for preventive measures, it is crucial to incorporate the opinions and behaviors of the population when modeling the impact of these measures on malaria transmission. The opinions and behaviors of the population have often been overlooked in previous studies. A mathematical model that accounts for these factors may yield different results than models ignoring them, highlighting the importance of understanding how public opinions and behaviors influence malaria prevention, transmission, and morbidity [8]. Recent studies have investigated how opinions affect disease spread and herd immunity [9, 10, 11]. Most of this research focuses on vaccination, a specific type of prophylactic behavior. Other preventive actions, such as hand washing, wearing face masks, or maintaining social distancing, differ because they require frequent and repeated engagement; for instance, hands must be washed after contact with potentially contaminated surfaces, and face

masks should be worn daily [12]. Consequently, opinion dynamics around vaccination differ from those around other preventive behaviors. Understanding the interactions between opinions, behaviors, and disease spread is therefore essential. Models combining opinion dynamics with seasonal compartmental frameworks provide valuable insights, though challenges remain due to assumptions and simplifications in representing population behavior [13, 14]. Many epidemic models focus on vaccination opinions [15, 16, 17], which have consistently raised safety and usage debates [18], while opinions on other preventive measures have received less attention despite their direct effects on transmission dynamics and attitudes toward vaccination [12]. Recent models integrating disease, economic factors, and opinion dynamics allow more realistic simulations of health beliefs, public health decisions, and disease progression [19, 20, 21]. Most models use simplified frameworks such as SIS [20, 22, 23], SIR [12, 19, 24], or SEIV [25]. However, existing malaria models rarely integrate behavioral or opinion dynamics, potentially underestimating the social drivers of disease transmission.

This study aims to fill this gap by examining how public opinions and behaviors influence malaria prevention methods, transmission, and disease burden. The main objective of this study is to model the impact of the population's opinions and behaviors regarding malaria prevention measures on malaria transmission and burden in 4 selected districts (Bembèrèkè, Nikki, N'Dali, and Sinendé) in the northern part of Benin. Specifically, we (i) assessed the impacts of the initial distribution of behaviors on malaria transmission and burden and (ii) examined the impacts of the nature of behavioral responses on malaria transmission and burden.

2. METHODS

Model formulation

We extend the model developed by [26] to account for opinion dynamics using an attitude spectrum [27]. The model considers two populations: human and mosquito populations. The human population is divided into susceptible humans (S), exposed humans (E_h), infectious humans (with minor symptoms, I_{uh}, asymptomatic, I_{ah} and symptomatic, I_{sh} individuals), hospitalized humans (H_h) and recovered humans (R_h). The mosquito population is divided into susceptible mosquitoes (S_m), exposed mosquitoes (E_m), and infectious mosquitoes (I_m). So, at time t, the

total population of humans is

$N_h(t) = S(t) + E_h(t) + I_{uh}(t) + I_{ah}(t) + I_{sh}(t) + H_h(t) + R_h(t)$.

For the simplicity of the model, we assume that opinion dynamics only occur within the susceptible human population each split into three groups, characterized by a given attitude in the attitude spectrum:

$$\mathbb{E} = \{-1; 0; 1\}. \tag{1}$$

Let's consider S_i as a susceptible human population with attitude i, for any $i \in \mathbb{E}$. For instance, S_{-1} are susceptible humans with high levels of prophylactic preventive attitudes (those who use insecticide-treated bed-Nets (ITNs) and indoor residual spraying or other preventive methods), S_1 are susceptible humans with a low level of prophylactic preventive attitudes and S_0 are susceptible humans with intermediate prophylactic preventive attitudes. Therefore, at time t, the population of susceptible humans is given by: $S(t) = \sum_{i \in \mathbb{E}} S_i(t)$.

Using the approach by [12], implemented by [28] on COVID-19 dynamics, we introduce the rate Ω_i at which a susceptible individual, S_i influences the rest of the susceptible population, which is called the influence function. We suppose the influence function Ω_i depends on the prevalence of the disease at time t:

$$P(t) = \frac{I_{ah}(t) + I_{uh}(t) + I_{sh}(t) + H_h(t)}{N_h(t)}.$$

Then, $\Omega_i(t) = \Omega_i(\tilde{P}(t))$, where, $\tilde{P}(t)$ the estimate of $P(t)$ reported by the mass media and Ω_i can be Linear or Saturating or fixed order saturating or Reverse-order Saturating defined on $[0, 1]$.

In the model developed by [12], the population is divided into four attitude groups, S_{-2}, S_{-1}, S_1, S_2, each associated with an influence function $\omega_i(I)$, which depends on the disease prevalence $I(t)$. The simplication considered in section (1) leads to: $i = -1$ (individuals with strong prophylactic attitudes), $i = 0$ (individuals with intermediate prophylactic attitudes), and $i = 1$ (individuals with weak or no prophylactic attitudes).

This simplification is based on the assumption that the group $i = 0$ in the model represents a behavioral average of the two intermediate groups (S_{-1} and S_1) in the original Tyson framework. This allows for a more interpretable and context-appropriate representation of behavior in our

study population. We adapted the influence functions developed by [12] to account for the three attitude groups considered (Table 1).

TABLE 1. Four types of influence functions $\Omega_i(y)$ adapted to our three-group framework.

$\Omega_i(y)$	**Linear**	**Saturating**	**Fixed-order Saturating**	**Reverse-order Saturating**
$i=-1$	$\Omega_0\left(1+\frac{1}{2}\Omega_{\max}y\right)$	$\Omega_0\left(1+\frac{1}{2}\Omega_{\max}\frac{y}{m+y}\right)$	$\Omega_0\left(1+\frac{1}{2}\Omega_{\max}\frac{y}{m+y}\right)$	$\Omega_0\left(1+\Omega_{\max}\frac{y}{m+y}\right)$
$i=0$	$\Omega_0\left(1+\frac{\Omega_{\max}-1}{4}y\right)$	$\Omega_0\left(1+\frac{\Omega_{\max}-1}{4}\frac{y}{m+y}\right)$	$\Omega_0\left(1+\frac{\Omega_{\max}-1}{4}\frac{y}{m+y}\right)$	$\Omega_0\left(1+\frac{\Omega_{\max}-1}{2}\frac{y}{m+y}\right)$
$i=1$	$\Omega_0\left(1-\frac{1}{2}y\right)$	$\Omega_0\left(1-\frac{1}{2}\frac{y}{m+y}\right)$	$\Omega_0\left(1-\frac{1}{2}\frac{y}{m+y}\right)$	$\Omega_0\left(1+\frac{y}{m+y}\right)$

For the Reverse-order saturating case, we adopt as the baseline in this study, the mathematical formulation is given by:

$$\Omega_i(y)=\begin{cases}\Omega_0\left[1+\Omega_{\max}\dfrac{y}{m+y}\right], & \text{if } i=-1,\\ \Omega_0\left[1+\dfrac{(\Omega_{\max}-1)}{2}\dfrac{y}{m+y}\right], & \text{if } i=0,\\ \Omega_0\left[1-\dfrac{y}{m+y}\right], & \text{if } i=1,\end{cases} \tag{2}$$

where Ω_0 ($\Omega_0 \geq 0$) is the baseline influence rate representing the influence in the absence of disease, $\Omega_{\max}$ ($\Omega_{\max} \geq 1$) is the maximum influence level for highly prophylactic individuals, describing the highest level of behavioral influence exerted by highly prophylactic individuals when disease awareness is at its peak, and m ($m \geq 0$) is a half-saturation constant, indicating the level of perceived disease prevalence at which the influence rate reaches half of its maximum.

In the rest of the study, we consider all four types of influence functions to investigate how the nature of behavioral response affects the disease transmission dynamics.

In the susceptible human group, when an S_i individual influences S_j individual, the attitude of the influenced individual is updated in one of the following ways:

- the individual S_j moves one step towards i ($S_j \to S_0$) if $j=-i$ with $j\neq 0$, and keep its opinion if $j=i$.

- the individual S_j moves one step towards i ($S_0 \to S_i$) if $j = 0$ and $i = \pm 1$.

Changes of opinions and prophylactic attitudes in the susceptible human population are expressed by the rate $\chi_{(i,j)}(t)$ ($i \to j$), which are defined as follows:

$$\chi_{(-1,0)}(t) = \frac{\Omega_0(t)S_0(t) + \Omega_1(t)S_1(t)}{N_h(t)}, \tag{3}$$

$$\chi_{(0,-1)}(t) = \frac{\Omega_{-1}(t)S_{-1}(t)}{N_h(t)}, \tag{4}$$

$$\chi_{(0,1)}(t) = \frac{\Omega_1(t)S_1(t)}{N_h(t)}, \tag{5}$$

$$\chi_{(1,0)}(t) = \frac{\Omega_0(t)S_0(t) + \Omega_{-1}(t)S_{-1}(t)}{N_h(t)}. \tag{6}$$

The specific forces of infection λ_{-1h}, λ_{0h} and λ_{1h} for susceptible humans, S_{-1}, S_0 and S_1 respectively are given by:

$$\lambda_{-1h}(t) = \frac{\psi^2 \beta b_h I_m}{N_h}, \lambda_{0h}(t) = \frac{\psi \beta b_h I_m}{N_h} \quad \text{and} \quad \lambda_{1h}(t) = \frac{\beta b_h I_m}{N_h},$$

where b_h, the rate at which a bite from infectious mosquitoes on susceptible humans will lead to infection of humans, β, the mosquito biting rate and the parameter ψ ($0 \leq \psi \leq 1$) reflecting the reduction in the force of infection due to prophylactic attitudes. Thus, the force of infection for the human population is given by the average:

$$\bar{\lambda}_h(t) = \frac{1}{S(t)} \sum_{i \in \mathbb{E}} S_i(t)\lambda_{ih}(t). \tag{7}$$

The force of infection for mosquitoes, λ_{hm} is given by:

$$\lambda_{hm}(t) = \frac{\beta \left(p_a I_{ah}(t) + p_u I_{uh}(t) + p_s I_{sh}(t) \right)}{N_h(t)}, \tag{8}$$

where p_a, p_u, and p_s are the probabilities that a bite from susceptible mosquitoes on infectious humans (asymptomatic individuals, infectious humans with minor symptoms, and asymptomatic individuals, respectively) leads to the infection of mosquitoes.

The biting rate β is given by:

$$\beta = \frac{EIR}{n_0 \cdot p_m}, \tag{9}$$

where, EIR is the entomological inoculation rate, n_0 is the mosquito-to-human density ratio ($n_0 = \frac{N_m}{N_h}$), and p_m is the proportion of mosquitoes infected by the parasite.

Seasonality is incorporated by allowing the birth rate of mosquitoes (b) to fluctuate periodically over time. Following the approach in [26], we assume that $b(t)$ varies sinusoidally with period T:

$$b(t) = b_0\left(1+\alpha_1 \sin\left(\frac{2\pi}{12}\left(t - t_{\max} + 3\right)\right)\right), \tag{10}$$

where α_1 is the amplitude of the seasonal variation ($0 \leq \alpha_1 \leq 1$), t_{max} is the peak month of the rainfall, and b_0 is the baseline value of the mosquito birth rate. Therefore, the number of newborn mosquitoes is given by:

$$\Lambda_m(t) = N_m \times b(t) \tag{11}$$

The flowchart of the model is presented in Figure 1, and the description of model parameters and state variables are presented in Table 2 and Table 3, respectively.

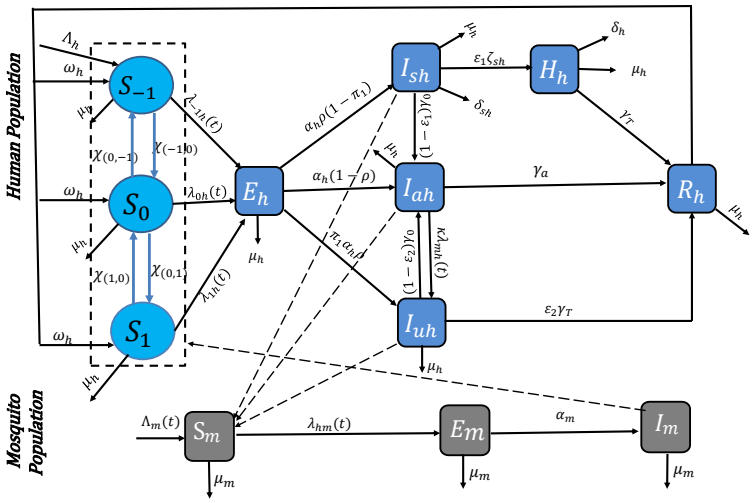

FIGURE 1. Susceptible humans (S) are divided into three classes according to their prophylactic preventive attitude; the indice $i \in \{-1,0,1\}$ indicate the level of prophylactic preventive attitude ($i=-1$ is the high level of prophylactic preventive attitude, $i=1$ is the low level of prophylactic preventive attitude and $i=0$ is the level of partial prophylactic preventive attitude); E_h, I_{ah}, I_{uh}, I_{sh}, H_h, R_h, S_m, E_m, I_m are respectively exposed humans, Asymptomatic humans, Infectious with minor symptoms, Symptomatic humans, Humans under treatment, Recovered humans, Susceptible mosquitoes, Exposed mosquitoes and Infectious mosquitoes.

TABLE 2. Definition of state variables of the model

State variables	Description
S_{-1}	Susceptible humans with high level of prophylactic preventive attitude
S_0	Susceptible humans with a middle level of prophylactic preventive attitude
S_1	Susceptible humans with a low level of prophylactic preventive attitude
E_h	Exposed humans
I_{uh}	Infectious humans with minor symptoms
I_{ah}	Asymptomatic humans
I_{sh}	Symptomatic humans
H_h	Hospitalized humans
R_h	Recovered humans
S_m	Susceptible mosquitoes
E_m	Exposed mosquitoes
I_m	Infectious mosquitoes

Ordinary differential equations

Using the flowchart of the model framework (Figure 1) and the above description, we obtain the following Ordinary Differential Equations (ODEs) of the model:

$$\dot{S}_{-1} = \Lambda_h + p_1\omega_h R_h + \chi_{(0,-1)}S_0 - \left(\mu_h + \lambda_{-1h} + \chi_{(-1,0)}\right)S_{-1}, \tag{12a}$$

$$\dot{S}_0 = 0.5(1-p_1)\omega_h R_h + \chi_{(1,0)}S_1 + \chi_{(-1,0)}S_{-1} - \left(\mu_h + \lambda_{0h} + \chi_{(0,-1)} + \chi_{(0,1)}\right)S_0, \tag{12b}$$

$$\dot{S}_1 = 0.5(1-p_1)\omega_h R_h + \chi_{(0,1)}S_0 - \left(\mu_h + \lambda_{1h} + \chi_{(1,0)}\right)S_1, \tag{12c}$$

$$\dot{E}_h = \lambda_{-1h}S_{-1} + \lambda_{0h}S_0 + \lambda_{1h}S_1 - (\mu_h + \alpha_h)E_h, \tag{12d}$$

$$\dot{I}_{uh} = \pi_1\alpha_h\rho E_h + \kappa\lambda_{mh}(t)I_{ah} - \Big(\varepsilon_2\gamma_T + (1-\varepsilon_2)\gamma_0 + \mu_h\Big)I_{uh}, \tag{12e}$$

$$\dot{I}_{ah} = \alpha_h(1-\rho)E_h + (1-\varepsilon_1)\gamma_0 I_{sh} + (1-\varepsilon_2)\gamma_0 I_{uh} - (\gamma_a + \kappa\lambda_{mh}(t) + \mu_h)I_{ah}, \tag{12f}$$

$$\dot{I}_{sh} = \alpha_h \rho (1-\pi_1) E_h - \Big(\varepsilon_1 \zeta_{sh} + (1-\varepsilon_1)\gamma_0 + \mu_h + \delta_{sh}\Big) I_{sh}, \tag{12g}$$

$$\dot{H}_h = \varepsilon_1 \zeta_{sh} I_{sh} - \Big(\delta_h + \gamma_T + \mu_h\Big) H_h, \tag{12h}$$

$$\dot{R}_h = \gamma_a I_{ah} + \gamma_T H_h + \varepsilon_2 \gamma_T I_{uh} - (\omega_h + \mu_h) R_h, \tag{12i}$$

$$\dot{S}_m = \Lambda_m(t) - (\mu_m + \lambda_{hm}(t)) S_m, \tag{12j}$$

$$\dot{E}_m = \lambda_{hm}(t) S_m - (\mu_m + \alpha_m) E_m, \tag{12k}$$

$$\dot{I}_m = \alpha_m E_m - \mu_m I_m. \tag{12l}$$

The initial conditions

$S_i(0) \geq 0$, for any $i \in \mathbb{E}$, $E_h(0) \geq 0$, $I_{ah}(0) \geq 0$, $I_{uh}(0) \geq 0$, $I_{sh}(0) \geq 0$, $H_h(0) \geq 0$, $R_h(0) \geq 0$,

$S_m(0) \geq 0$, $E_m(0) \geq 0$, $I_m(0) \geq 0$.

TABLE 3. Definition of the parameters

Parameters	**Description**	**Unit**
Λ_h	Number of newborn humans in susceptible humans S_{-1}	month^{-1}
μ_h	Natural death rate in humans	month^{-1}
σ_h	Moving rate from exposed to infectious humans (I_{uh} or I_{ah} or I_{sh})	month^{-1}
ρ	Probability of symptomatic infection	dimensionless
π_1	Proportion of uncomplicated malaria	%
β	Biting rate of mosquitoes in susceptible human population	mosquito/human
b_h	Probability of disease transmission from mosquitoes to humans	dimensionless
δ_{sh}	Mortality rate of severe malaria	month^{-1}
δ_h	Mortality rate of hospitalized malaria cases	month^{-1}
γ_a	Recovery rate for asymptomatic humans, I_{ah}	month^{-1}

γ_T	Recovery rate for hospitalized humans, H_h	month^{-1}
ε_1	Treatment access coverage for severe malaria	%
ε_2	Treatment access coverage for uncomplicated malaria	%
ζ_{sh}	Admission rate to hospital for severe malaria	month^{-1}
ω_h	Waning rate of acquired immunity after recovery	month^{-1}
$b(t)$	Time-dependent mosquito birth rate	mosquito·month^{-1}
α_m	Progression rate from exposed to infectious mosquitoes	month^{-1}
μ_m	Mosquito mortality rate	month^{-1}
EIR	Entomological inoculation rate	mosquito/human
ψ	Percentage reduction of biting rate due to prophylactic attitude	%
α_1	Amplitude of seasonal variation	dimensionless
m	Half-saturation constant	dimensionless
Ω_0	Baseline influence rate	month^{-1}
Ω_{max}	Maximum influence strength	month^{-1}
p_1	Proportion of people adhering to prophylactic measures	%

Data source and study period

The four districts in the northern and central parts of Benin (Bantè, Dassa, Sinendé, and Tchaourou) were considered for this study due to the availability of the data (Figure 5). This study relied on secondary data obtained from the National Malaria Control Program (PNLP) of Benin. The data consist of monthly records of malaria cases and deaths (Figure 6). These were the most complete monthly records available from the PNLP, covering a five-year period from January 2019 to December 2023. In addition to malaria case and death data, this study incorporated opinion data extracted from [29], reporting the proportion of individuals adhering to malaria preventive measures in each of the selected districts. Specifically, adherence (p_1) was 75.6% in the Central zone districts (Bantè, and Dassa) and 52.9% in the Northern zone districts

(Sinendé, and Tchaourou). The total population used for each district is from the Yearbook of Civil Status Statistics in Benin 2022 [30].

3. RESULTS

3.1. Analytical results

Positivity and Boundedness of the Model Solutions

To ensure that the model is mathematically and biologically well-posed, we prove in this section that the solutions of the system remain positive and bounded for all $t \geq 0$, provided that the initial conditions are non-negative.

Let the state vector be denoted by:

$$X(t) = (S_{-1}(t), S_0(t), S_1(t), E_h(t), I_{uh}(t), I_{ah}(t), I_{sh}(t), H_h(t), R_h(t), S_m(t), E_m(t), I_m(t)).$$

We show that for all $t \geq 0$, $X(t) \in \mathbb{R}_+^{12}$, and the total human and mosquito populations are bounded.

Positivity of the solutions

We first show that the compartments remain positive for all $t \geq 0$.

Let us consider the equation for $S_{-1}(t)$: $\dot{S}_{-1} = \Lambda_h + p_1\omega_h R_h + \chi_{(0,-1)}S_0 - (\mu_h + \lambda_{-1,h} + \chi_{(-1,0)})S_{-1}$.

This can be written as: $\dot{S}_{-1} \geq -B(t)S_{-1}$, where $B(t) = \mu_h + \lambda_{-1,h} + \chi_{(-1,0)}$.

Using Gronwall's inequality, we get:

$$S_{-1}(t) \geq S_{-1}(0)\exp\left(-\int_0^t B(s)\,ds\right) \geq 0.$$

Hence, $S_{-1}(t) \geq 0$ for all $t \geq 0$, provided that $S_{-1}(0) \geq 0$.

Similarly, the equations for S_0 and S_1 can be written in the form:

$$\dot{S}_i(t) \geq -B_i(t)S_i(t),$$

which implies $S_0(t), S_1(t) \geq 0$ for all $t \geq 0$.

The exposed compartment E_h satisfies:

$$\dot{E}_h = \lambda_{-1,h}S_{-1} + \lambda_{0,h}S_0 + \lambda_{1,h}S_1 - (\mu_h + \sigma_h)E_h \geq -(\mu_h + \sigma_h)E_h.$$

Thus, $E_h(t) \geq 0$.

All other compartments $I_{uh}, I_{ah}, I_{sh}, H_h, R_h$ follow similar forms: $\dot{x}(t) \geq -B(t)x(t)$ which ensures their positivity.

Now, consider the mosquito compartments. The susceptible mosquito equation is:

$$\dot{S}_m = \Lambda_m(t) - (\mu_m + \lambda_{hm})S_m \geq -(\mu_m + \lambda_{hm})S_m.$$

So $S_m(t) \geq 0$.

The equations for E_m and I_m are:

$$\dot{E}_m = \lambda_{hm}S_m - (\mu_m + \alpha_m)E_m, \quad \dot{I}_m = \alpha_m E_m - \mu_m I_m.$$

By similar reasoning, $E_m(t), I_m(t) \geq 0$.

Boundedness of the solutions

Let the total human population be: $N_h(t) = S_{-1} + S_0 + S_1 + E_h + I_{uh} + I_{ah} + I_{sh} + H_h + R_h$.

Then,

$$\dot{N}_h = \Lambda_h - \mu_h N_h - \delta_{sh} I_{sh} - \delta_h H_h \leq \Lambda_h - \mu_h N_h.$$

Applying Gronwall's inequality, we obtain:

$$N_h(t) \leq \frac{\Lambda_h}{\mu_h} + \left(N_h(0) - \frac{\Lambda_h}{\mu_h}\right) e^{-\mu_h t} \Rightarrow \lim_{t\to\infty} N_h(t) \leq \frac{\Lambda_h}{\mu_h}.$$

Similarly, let:

$$N_m(t) = S_m + E_m + I_m.$$

Then, $\dot{N}_m = \Lambda_m(t) - \mu_m N_m \leq \Lambda_m^{\max} - \mu_m N_m$ where $\Lambda_m^{\max} = \sup_{t\geq 0} \Lambda_m(t)$.

It follows that:

$$N_m(t) \leq \frac{\Lambda_m^{\max}}{\mu_m} + \left(N_m(0) - \frac{\Lambda_m^{\max}}{\mu_m}\right) e^{-\mu_m t} \Rightarrow \lim_{t\to\infty} N_m(t) \leq \frac{\Lambda_m^{\max}}{\mu_m}.$$

Then, $N_h(t) \leq \frac{\Lambda_h}{\mu_h}$, $N_m(t) \leq \frac{\Lambda_m^{\max}}{\mu_m}$. Therefore, all state variables are bounded.

Disease-free periodic solution

To determine the existence of a disease-free periodic solution (X^0), we set the rate of change for each compartment to zero, assuming there is no infection within the population. At the DFE, all infectious compartments and the derivative of all state variables are zero, denoted as Then, the disease-free periodic solution X^0 of the model (12a)-(12l) is expressed as:

$$\left(E_h^0, I_{uh}^0, I_{ah}^0, I_{sh}^0, H_h^0, E_m^0, I_m^0, S_{-1}^0, S_0^0, S_1^0, R_h^0, S_m^0(t)\right) = \left(0,0,0,0,0,0,0,S_{-1}^0, S_0^0, S_1^0, 0, S_m^0(t)\right),$$

where $S_m^0(t)$ is the solution of the differential equation:

$$\dot{S}_m^0(t) = \Lambda_m(t) - \mu_m S_m^0(t), \tag{13}$$

and S_{-1}^0, S_0^0, S_1^0 are the solution of the following system:

$$\begin{cases} \Lambda_h - \left(\mu_h + \dfrac{\Omega_0 S_1^0}{N_h^0}\right) S_{-1}^0 = 0, \\ \dfrac{2\Omega_0 S_1^0 S_{-1}^0}{N_h^0} - \mu_h S_0^0 = 0, \\ -\left(\mu_h + \dfrac{\Omega_0 S_{-1}^0}{N_h^0}\right) S_1^0 = 0. \end{cases} \tag{14}$$

Since Λ_m is periodic with period T, then the equation (13) has a T-periodic solution defined by:

$$S_m^0(t) = \left[S_m(0) + \int_0^t \Lambda_m(r) e^{r\mu_m}\, dr \right] e^{-t\mu_m}, \tag{15}$$

where

$$S_m(0) = \frac{\int_0^T \Lambda_m(r) e^{r\mu_m}\, dr}{e^{t\mu_m} - 1}.$$

Then, the total population of humans and mosquitoes at X^0 is given respectively by

$$N_h^0 = S_{-1}^0 + S_0^0 + S_1^0 = S_h^0, \quad N_m^0 = S_m^0.$$

After solving the system of equation 14, we now have:

$$\begin{cases} S_{-1}^0 = \dfrac{\Lambda_h}{\mu_h}, \\ S_0^0 = 0, \\ S_1^0 = 0. \end{cases} \tag{16}$$

Control and Effective Reproduction Numbers

We define the key epidemiological metric associated with system (12a)–(12l), defined as the control reproduction number R_c. Several methods have been developed to compute this threshold quantity, notably the next-generation matrix approach for autonomous systems [31] and

its extensions to periodic or non-autonomous models [32]. In the present study, we apply this framework to our non-autonomous malaria model to determine the conditions under which the disease can persist or die out. Therefore, the system (12a) – (12l) can be rewritten as:

$\dot{X}(t) = (f(t) - v(t))X(t)$, where, $X(t) = (E_h(t), I_{uh}(t), I_{ah}(t), I_{sh}(t), H_h(t), E_m(t), I_m(t))$, and

$$f(t) = \begin{pmatrix} \lambda_{-1h}S_{-1} + \lambda_{0h}S_0 + \lambda_{1h}S_1 \\ 0 \\ 0 \\ 0 \\ 0 \\ \lambda_{hm}(t)S_m \\ 0 \end{pmatrix},$$

$$v(t) = \begin{pmatrix} (\mu_h + \alpha_h)E_h \\ -\pi\alpha_h\rho E_h - \kappa\lambda_{mh}(t)I_{ah} + (\varepsilon_2\gamma_T + (1-\varepsilon_2)\gamma_0 + \mu_h)I_{uh} \\ -\alpha_h(1-\rho)E_h - (1-\varepsilon_1)\gamma_0 I_{sh} - (1-\varepsilon_2)\gamma_0 I_{uh} + (\gamma_a + \kappa\lambda_{mh}(t) + \mu_h)I_{ah} \\ -\alpha_h\rho(1-\pi)E_h + (\varepsilon_1\zeta_{sh} + (1-\varepsilon_1)\gamma_0 + \mu_h + \delta_{sh})I_{sh} \\ -\varepsilon_1\zeta_{sh}I_{sh} + (\delta_h + \gamma_T + \mu_h)H_h \\ (\mu_m + \alpha_m)E_m \\ -\alpha_m E_m + \mu_m I_m \end{pmatrix}.$$

Let set $F(t) = \left(\frac{\partial f(t)}{\partial X(t)}\right)$ and $V(t) = \left(\frac{\partial v(t)}{\partial X(t)}\right)$ the Jacobian matrix of $f(t)$ and $v(t)$ at X^0. Then, we have:

$$F(t) = \begin{pmatrix} 0 & 0 & 0 & 0 & 0 & 0 & y \\ 0 & 0 & 0 & 0 & 0 & 0 & 0 \\ 0 & 0 & 0 & 0 & 0 & 0 & 0 \\ 0 & 0 & 0 & 0 & 0 & 0 & 0 \\ 0 & \frac{\beta p_u S_m^0}{N_h^0} & \frac{\beta p_a S_m^0}{N_h^0} & \frac{\beta p_s S_m^0}{N_h^0} & 0 & 0 & 0 \\ 0 & 0 & 0 & 0 & 0 & 0 & 0 \\ 0 & 0 & 0 & 0 & 0 & 0 & 0 \end{pmatrix},$$

where $y = \dfrac{\beta b_h (S_1^0 + \psi S_0^0 + \psi^2 S_{-1}^0)}{N_h^0} = \beta b_h \psi^2$, and

$$V(t) = \begin{pmatrix} \mu_h + \alpha_h & 0 & 0 & 0 & 0 & 0 & 0 \\ -\pi_1 \alpha_h \rho & x_1 & 0 & 0 & 0 & 0 & 0 \\ -\alpha_h(1-\rho) & -(1-\varepsilon_2)\gamma_0 & \mu_h + \gamma_a & -(1-\varepsilon_1)\gamma_0 & 0 & 0 & 0 \\ -\alpha_h \rho (1-\pi_1) & 0 & 0 & x_2 & 0 & 0 & 0 \\ 0 & 0 & 0 & -\varepsilon_1 \zeta_{sh} & \mu_h + \gamma_T + \delta_h & 0 & 0 \\ 0 & 0 & 0 & 0 & 0 & \mu_m(t) + \alpha_m & 0 \\ 0 & 0 & 0 & 0 & 0 & -\alpha_m & \mu_m(t) \end{pmatrix},$$

where $x_1 = \varepsilon_2 \gamma_T + (1-\varepsilon_2)\gamma_0 + \mu_h$ and $x_2 = \mu_h + \varepsilon_1 \zeta_{sh} + (1-\varepsilon_1)\gamma_0 + \delta_{sh}$.

Let C_T be an ordered Banach space of all T–periodic functions from $\mathbb{R}$ to $\mathbb{R}$ and C_T^+ the positive cone $\left(C_T^+ = \{g \in C_T / g(t) \geq 0, t \in \mathbb{R}\}\right)$. Let $\Gamma(s) = (E_h(s), I_{uh}(s), I_{ah}(s), I_{sh}(s), H_h(s), E_m(s), I_m(s))'$ be the initial distribution of the infected population introduced at time s. Then, $F(s)\Gamma(s)$ is the distribution of newly infected individuals caused by the infected individuals introduced at time s. Therefore, $Y(t,s)F(s)\Gamma(s)$ is the distribution of the infected individuals newly infected at time s and remained in infection compartments at time t, where $Y(t,s)$ is the evolution operator solution of the following linear system:

$$\frac{dY(t,s)}{dt} = -V(t)Y(t,s), \quad t \geq s, \quad Y(s,s) = I_7.$$

Hence, the distribution of the accumulated value of new infections at time t caused by the infected individuals introduced at time s is given by:

$$\psi(t) = \int_{-\infty}^{t} Y(t,s)F(s)\Gamma(s)\,ds.$$

By setting $q = t - s$, we have:

$$\psi(t) = \int_{0}^{\infty} Y(t,t-q)F(t-q)\Gamma(t-q)\,dq.$$

According to [33, 34, 35], the basic reproduction number R_0 of the model (12a) – (12j) is the spectral radius of the next-generation operator $L : C_T \longrightarrow C_T$ given by:

$$(L\Gamma)(t) = \int_{0}^{\infty} Y(t,t-q)F(t-q)\Gamma(t-q)\,dq.$$

It follows that the spectral radius of the next-generation operator L is not easy to find. Therefore, to find the control reproduction number of the model, we will use the monodromy matrix method as in [34, 35].

Let $W(t,\lambda)$ be the evolution operator of the T–periodic system:

$$\frac{dW}{dt} = \left(\frac{1}{\lambda}F(t) - V(t)\right)W, \quad \text{where } t \in \mathbb{R} \text{ and } \lambda > 0.$$

According to Theorem 3.1 in [36], the control reproduction number of the model is the unique solution λ of the equation

$$\rho(W(t,\lambda)) = 1,$$

where $\rho(W(t,\lambda))$ is the spectral radius of the matrix $W(t,\lambda)$. Therefore, the model's control reproduction number R_c will be found numerically such that $\rho(W(t,R_c)) = 1$.

Using the numerical method, we followed the following algorithm (E) to compute the control reproduction number of the model.

The effective reproduction number R_f of the model is defined as:

$$R_f(t) = R_0 \times \frac{S_{-1}(t) + S_0(t) + S_1(t)}{N_h(t)},$$

where R_0 represents the basic reproduction number, that is, the reproduction number in the absence of any control measures.

3.2. Numerical analyses

This section presents the numerical analysis based on the number of malaria cases collected from January 2019 to December 2023, covering 4 districts in Benin: Bantè, Dassa, Sinendé, and Tchaourou. These data were obtained from the National Malaria Control Program of Benin(PNLP) and serve as the empirical basis for the simulations and evaluations conducted in this study. The parameters extracted from the literature are summarized in Table 4.

The trends in malaria cases and deaths for each district are illustrated through graphs provided in the appendix (Figure 6), offering a visual overview of the temporal dynamics over the five years.

Parameter estimation

The estimation of model parameters was performed using both values extracted from the literature and values obtained through numerical calibration based on the real-world malaria data described earlier. The following parameters were estimated (Table 5) using the observed data on malaria cases: δ_{sh}, α_1, ψ, ε, m, Ω_{max}, EIR and ζ_{sh}. The model was numerically solved using the MATLAB function `ode45`, which integrates systems of ordinary differential equations (ODEs). The estimation process was carried out using the *non-linear least squares method*, a widely used technique for minimizing the difference between model outputs and observed data. This technique was implemented in MATLAB using the `fminsearchbnd` function, which extends `fminsearch` by allowing bounded minimization of multivariable functions.

To assess the accuracy of the parameter estimates, we computed the Root Mean Squared Error (RMSE), defined as:

$$\text{RMSE} = \sqrt{\frac{1}{n}\sum_{i=1}^{n}\left(y_i^{\text{obs}} - y_i^{\text{pre}}\right)^2},$$

where y_i^{obs} and y_i^{pre} are the observed and predicted values, respectively, and n is the number of time points. A smaller RMSE value indicates better model performance and more accurate parameter estimation [37]. To avoid local minima and improve robustness, initial parameter values were simulated in 100 different sets from predefined intervals using the MATLAB function `datasample`. The combination of nonlinear least squares optimization, repeated sampling, and RMSE-based evaluation provides a sound and widely adopted framework for parameter estimation in infectious disease modeling [38, 39]. The curves showing the results of the model calibration for each of the 4 study districts are presented in Figure 7. From this figure, for each location, the monthly reported malaria cases (blue circles) are plotted alongside the predicted values obtained from the calibrated model (red line), covering the period from January 2019 to December 2023.

TABLE 4. Parameter values extracted from the literature

Parameters	Baseline Value Used	Range	Unit	Source
μ_h	0.0079	–	month^{-1}	Calculated from [40]
b_h	0.0031	–	month^{-1}	Calculated from [40]
π_1	0.5	[0–1]	%	Assumed
κ	0.5	[0–1]	%	Assumed
ρ	0.5	[0–1]	%	Assumed
γ_0	0.168	[0.042–0.51]	month^{-1}	[41]
γ_a	0.1065	[0.042–0.51]	month^{-1}	[41]
α_h	3	[2.01–6]	month^{-1}	[41]
γ_T	1.216	[0–6]	month^{-1}	[42]
ω_h	0.0304	[0.00165–0.33]	month^{-1}	[41]
ε_1	0.3993	[0–1]	%	Computed from [1]
ε_2	0.3993	[0–1]	%	Computed from [1]
p_u	0.03	[0.0072–0.64]	dimensionless	[42]
p_a	0.03	[0.0072–0.64]	dimensionless	[42]
p_s	0.4	[0.072–0.64]	dimensionless	[42]
ζ_{sh}	0.0042	[0–2.5]	month^{-1}	Computed from [42]
n_0	10	[5–30]	mosquito/human	Assumed
p_m	0.05	[0–1]	dimensionless	Assumed
Λ_{m0}	3.9542	[0.06–6000]	mosquito·month^{-1}	[42]
b_m	0.1	[0.01–0.27]	dimensionless	[41]
α_m	3.04	[0.87–9.9]	month^{-1}	[41]
μ_m	1.689	[1–3.03]	month^{-1}	[41]

$\Lambda_h = Population \times b_h$.

TABLE 5. Parameter estimates and root mean square error (RMSE) across districts

Parameters	Bantè	Dassa	Sinendé	Tchaourou
δ_{sh}	0.001 [0.000–0.003]	0.000 [0.000–0.002]	0.005 [0.000–0.012]	0.043 [0.039–0.047]
α_1	0.958 [0.916–1.000]	1.000 [0.978–1.022]	0.999 [0.847–1]	0.898 [0.833–0.963]
ψ	0.479 [0.398–0.559]	0.967 [0.857–1.000]	0.569 [0.367–0.772]	0.335 [0.191–0.479]
ε	0.102 [0.093–0.110]	0.178 [0.156–0.201]	0.494 [0.434–0.554]	0.380 [0.319–0.441]
m	155.622 [141.453–169.792]	101.507 [89.166–113.849]	20.902 [10.872–30.932]	14.884 [1.456–28.313]
$\Omega_{\max}$	59.886 [52.961–66.811]	6.182 [0.000–12.781]	19.616 [0.000–43.858]	16.231 [9.481–22.981]
EIR	99.708 [96.817–102.599]	98.254 [94.856–101.653]	17.886 [1.753–34.018]	35.032 [18.622–51.443]
ζ_{sh}	0.027 [0.025–0.029]	0.102 [0.076–0.129]	0.980 [0.976–0.984]	0.980 [0.979–0.981]
RMSE	10381	4702	8840	26376

Effect of percentage reduction of force of infection on the control reproduction number

The figures 8a–8d illustrate how the control reproduction number R_c varies as a function of the percentage reduction of force of infection of the parameter, ψ, which represents the multiplication factor to reduce the infection risk among individuals who adopt preventive measures. For each district, R_c is plotted across a range of ψ values from 0 (full reduction: no infection occurs meaning that all individuals adopt perfect prophylactic behavior) to 1 (no reduction: no change in behavior meaning that the probability of infection remains the same as b_0), with the critical threshold $R_c = 1$ marked by a red dashed line. A smaller value of ψ leads to a greater reduction in disease transmission. A larger ψ (closer to 1) means that protective measures are less effective and the transmission rate remains relatively high.

The analysis of the figures shows a strong inverse relationship between ψ and R_c: as individuals adopt more effective prophylactic behavior, the control reproduction number decreases. This finding implies that improving adherence to vector control measures, specifically ITNs and topical repellents, may lead to meaningful reductions in malaria transmission at the community level. Across most districts, the red threshold line at $R_c = 1$ is crossed when ψ reaches a certain value, indicating the minimum level of prophylactic effectiveness required to control the outbreak. Notable differences are observed among districts. The districts are grouped into two distinct categories based on the level of effectiveness required: three districts (Bantè,

Dassa, and Sinendé) require the highest effectiveness, with a ψ value of 0.08, 0.12 and 0.16 respectively. This means that a reduction of at least 92%, 88% and 84% respectively in the probability of infection, respectively, is required to stop the epidemic, highlighting the intensity of baseline transmission in these areas. Conversely, Tchaourou requires the lowest effectiveness ($\psi = 0.4$), implying that a reduction of 60% is sufficient to manage the disease. These differential thresholds provide specific performance targets for optimizing prophylactic interventions in each community.

Impact of the initial proportion of favorable prophylactic attitudes on effective reproduction number across districts

The figures 2a–2d show the trends of the effective reproduction number from January 2019 to December 2023 across the four districts under five levels of favorable prophylactic opinion percentages (p_1).

Data from all districts show a clear trend: as the proportion of adherence to prophylactic measures increases, the effective reproduction number decreases over time. Specifically, for each level of favorable adherence, the effective reproduction number tends to decrease as the proportion of favorable adherent individuals increases. The districts show greater reductions, particularly for increased adherence (52% to 100%). Bantè and Dassa stand out with the most pronounced decline, with a decrease in $R_f(t)$ from 2.9 to 0.5 (a reduction of nearly 82.75%), highlighting the significant impact of behavioral interventions in areas of maximum transmission. These results confirm that adherence is universally effective, but that its marginal effect is amplified in regions with high epidemic dynamics.

Effect of opinions and influence on malaria clinical cases

The figures 3a–3d show the impact of opinion dynamics and influence on malaria transmission across the 4 districts. Based on these figures, across all districts, we remark that when there is no opinion, we see that the number of malaria clinical cases increases, and the epidemic takes longer to reach its peak. In this scenario, the number of cases is amplified, and the overall transmission remains high over an extended period. This means that without any collective belief or behavioral change in the population, the disease spreads more easily and for a longer duration, leading to a delayed response to the outbreak. In contrast, when opinion is present,

individuals are more likely to adopt preventive behaviors. This leads to a faster peak, indicating that the disease is controlled more quickly. As a result, the epidemic does not last as long, and the community can implement intervention strategies at a more opportune time, making it easier to manage the spread of the disease.

For instance, in the absence of public opinion, the number of malaria clinical cases in Dassa (Figure 3b) is around 3,600. When public opinion is present but without, the number of clinical cases decreases to around 1,600. This indicates that without public opinion, the epidemic progresses more slowly, and cases accumulate over a prolonged period. In contrast, when public opinion is present, the epidemic reaches its peak much earlier, in september 2019. The curve shows a sharp increase, but the peak is much lower compared to the "no opinion" scenario. The presence of public opinion accelerates the adoption of preventive behaviors, enabling quicker control and reducing the overall burden of the epidemic.

In addition, when public opinion is present but there is no influencing mechanism (red curve), the epidemic evolves in the same way as in the scenario without public opinion, although the number of clinical cases is slightly lower. This shows that even if individuals have opinions, without social influence, the adoption of preventive measures is slower. The epidemic reaches its peak in a delayed manner, and the control remains difficult. When social influence is introduced, we observe a significant change in the trends. The curve blue represents the presence of influence and show that the peak occurs earlier, and the overall number of clinical cases is substantially reduced. This indicates that social influence helps individuals adopt preventive behaviors more rapidly, leading to faster epidemic control.

Impact of the minimum Influence Rate Ω_0 on Effective Reproduction Number Across districts
The figures 4a– 4d show the effect of varying the minimum influence rate Ω_0 on effective reproduction number (2019–2023) in the four study districts. They reveal a clear negative relationship between the minimum influence rate Ω_0 and the effective reproduction number. As Ω_0 increases from 0.05 to 50, the effective reproduction number consistently decreases across all districts. This result highlights the importance of a strong underlying social influence, even in the absence of a visible disease burden. A higher Ω_0 means that protective opinions circulate more actively at all times, which encourages the continuous adoption of preventive behaviors.

The seasonal pattern of malaria transmission remains evident in all scenarios, but the amplitude of the peaks is noticeably reduced at higher Ω_0 values.

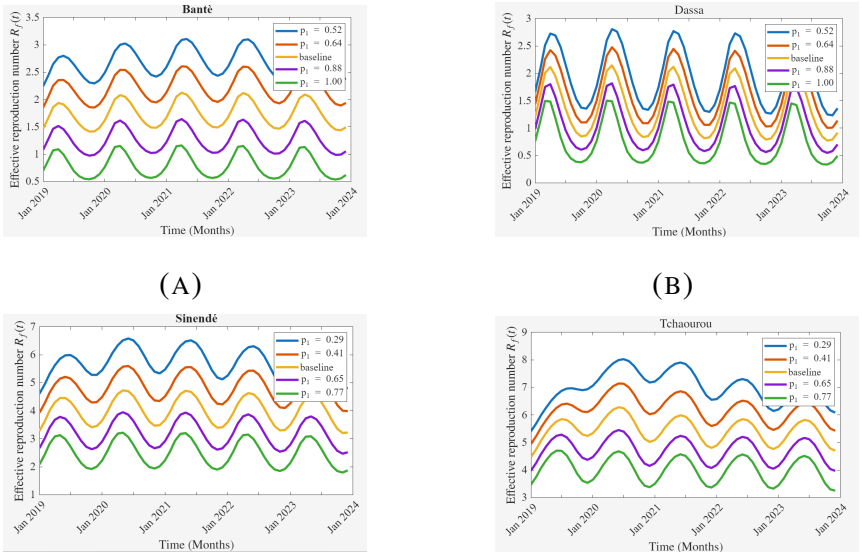

(A) (B)

(C) (D)

FIGURE 2. Effective Reproduction Number under various prophylaxis adherence levels across the four districts

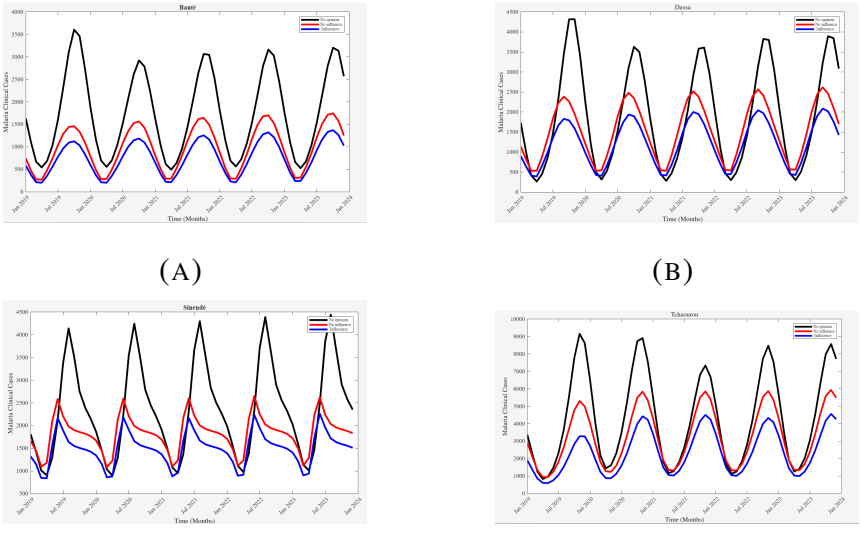

(A) (B)

(C) (D)

FIGURE 3. Malaria cases under various opinion and influence across the four districts

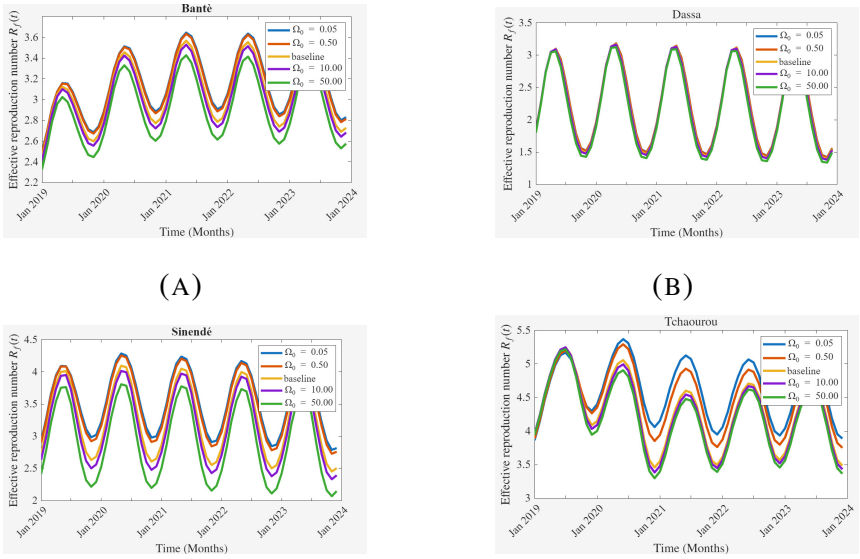

FIGURE 4. Effective reproduction number trends under varying minimum influence rate (Ω_0) across the four study districts

4. DISCUSSION

This study developed a seasonal malaria transmission model integrating public opinion and preventive behavior to quantify how social influence affects disease outcomes across 4 Beninese districts. Analytical results established positivity and boundedness, while numerical analyses revealed that opinion-driven adherence to preventive measures substantially reduced malaria incidence.

The simulations showed that as the level of favorable adherence to preventive measures increased, the effective reproduction number decreased consistently, highlighting the critical role of individual behavior in transmission dynamics. Simulation results showed also that the absence of protective opinions in the population led to higher and more sustained levels of malaria incidence across all districts. In contrast, when protective opinions were present at the beginning of the simulation, there was a clear reduction in both the size and frequency of malaria peaks. This confirms the significant contribution of opinion presence to the collective adoption of preventive behaviors. The model also accounted for how individuals influence one another based on their opinion type through influence function. This influence function was designed

to reflect the varying capacity of each group to affect others, with individuals who strongly prophylactic exerting the greatest influence. This structure, in which highly prophylactic individuals exert the greatest influence, follows the theoretical foundations proposed by [12]. It also aligns with a mechanism of opinion amplification whereby individuals with entrenched opinions tend to exert a stronger persuasive effect [27]. In addition, [28] supports the idea that pre-existing protective opinions can significantly alter epidemic trajectories, even in the absence of strong institutional interventions. The spread of awareness and information also plays a crucial role. This result is consistent with [43], who showed that awareness about an epidemic can spread through a population and modify individual behavior, potentially reducing transmission. In the present study, the behavioral changes driven by opinion diffusion had a similar effect, suggesting that even informal or peer-driven communication can lead to meaningful epidemiological outcomes. Furthermore, the results resonate with the work of [44], who modeled the co-dynamics of fear and disease. They demonstrated that perceived risk can lead individuals to withdraw from potential exposure, thereby reducing contact rates. Although the present model does not explicitly include fear, it captures the idea that perceived prevalence modulates behavior via opinion dynamics. Overall, these findings underscore the importance of incorporating social and behavioral components into epidemic models. Encouraging the spread of protective opinions through targeted communication or community-based interventions could enhance malaria prevention strategies, particularly in settings with limited access to medical infrastructure.

The behavioural response to prevention strategies was further examined through one key parameter of the influence function: the minimum influence rate (Ω_0). This parameter reflect how influence circulates in the population under normal conditions. Simulation results showed that higher values of Ω_0 were consistently associated with lower malaria incidence across all districts. This indicates that even in the absence of disease, a strong underlying influence structure promotes the adoption of protective behaviours. These findings align with [43], who emphasized that awareness can spread through social networks and lead to behavioral changes, even before the visible rise of infection. Similarly, [45] reported that perceived risk alone can lead to

significant behavioral adjustments in response to potential pandemics. As supported by [27], individuals with entrenched opinions are often more persuasive, especially within local networks. Therefore, strengthening the voice of committed individuals can significantly impact collective behaviour and reduce disease transmission. This echoes the importance of empowering community leaders or role models in public health campaigns. These findings reflect the insights of [44], who showed that delays in behavioural adaptation to fear or risk perception can amplify epidemic outcomes. Interestingly, the effects of each parameter varied slightly across districts, reflecting differences in initial conditions or transmission intensity. However, the overall trends remained consistent. These results also align with [28], who highlighted the importance of heterogeneity in behavioural dynamics and their consequences for regional epidemic control. Together, these findings emphasize that behavioural parameters are not only model components but also key levers for public health action. Interventions aimed at boosting baseline influence, empowering committed voices, and reducing behavioural inertia can have a measurable effect on malaria control. Despite the simplicity of the model, these insights offer valuable guidance for designing social and behavioural interventions that complement medical strategies.

Public health programs could benefit from leveraging community leaders and peer networks to promote sustained prophylactic behaviour, especially in high-risk or resource-limited settings. Future research could explore more complex network-based influence structures or integrate mobile data and real-time behavioural tracking. Such efforts would further enhance our capacity to model and control malaria transmission through a multidisciplinary lens that bridges epidemiology, sociology, and public health policy.

Despite the strengths of the study, some limitations must be acknowledged. The analysis was limited to four districts in Northern and Central Benin due to data availability. As a result, the findings may not fully represent the situation across the entire country. Future research could include more districts or adopt a spatial modeling approach to capture regional differences more accurately. Some parameters were assumed to remain constant over time and across locations. While this was necessary for model calibration, it does not reflect the potential influence of environmental or socio-economic variations. Future models could incorporate time-varying or climate-dependent parameters such as rainfall or temperature. Although the model integrates

public opinion, it does not include certain key interventions such as Seasonal Malaria Chemoprevention (SMC) or vaccination, mainly due to the lack of reliable data in the study areas. Including these strategies in future work could improve the model's relevance for guiding control programs. The model also does not account for challenges like drug resistance, unequal access to care, or climate change, which can affect malaria dynamics. Addressing these aspects in future studies would help build more effective and realistic tools for malaria control.

5. CONCLUSION

This study investigated the impact of population opinions and behavioural responses towards malaria prevention methods on the transmission dynamics and burden of malaria in four districts of Benin. By coupling the classical malaria transmission model with an opinion dynamics framework, this research aimed to provide a more holistic understanding of how individual attitudes and social influence mechanisms affect disease propagation. The results confirmed that opinions and behaviours are key determinants in shaping malaria transmission patterns. In particular, the initial distribution of prophylactic behaviours significantly influenced disease outcomes, with a higher initial proportion of favorable prophylactic individuals leading to a substantial reduction in malaria incidence. Moreover, the presence of opinion dynamics and influence consistently showed a mitigating effect on the disease spread, underscoring the power of social interactions in shaping health outcomes. This study emphasizes the impact of behavioral parameter such as minimum influence rate (Ω_0) on population responsiveness to the epidemic. High values of Ω_0 are associated with reduced transmission. These results confirm the importance of risk perception and social influence in behavioral adaptation, as spotlighted in previous work. One of the major contributions of this study lies in the contextualized application of an opinion-epidemic model to malaria, a vector-borne disease, in a sub-Saharan African setting, thus extending the work carried out on other diseases such as COVID-19.

APPENDICES

APPENDIX A. STUDY AREA MAP DISPLAYING THE 4 SELECTED DISTRICTS IN BENIN

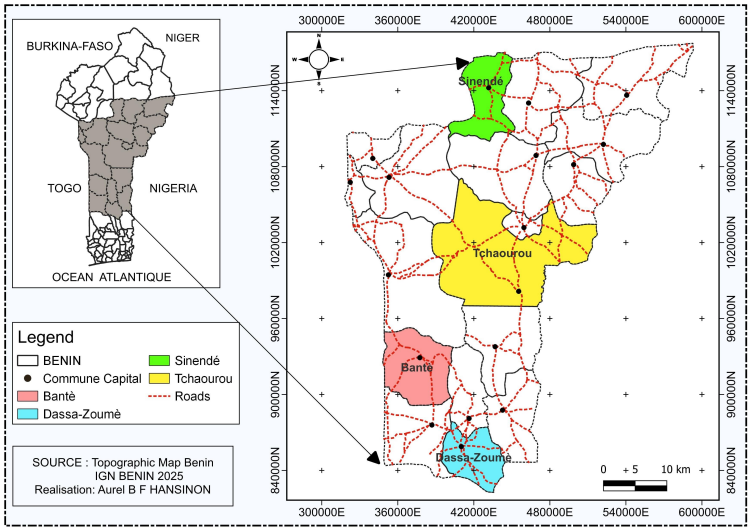

FIGURE 5. Study area map displaying the 4 selected districts in Benin

APPENDIX B. MONTHLY MALARIA DATA BY DISTRICT (2019–2023)

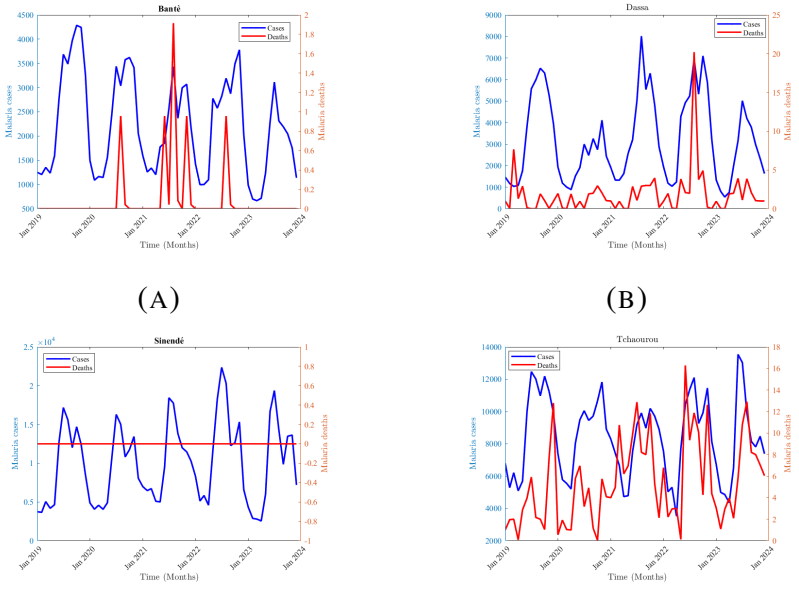

(A) (B)

(C) (D)

FIGURE 6. Malaria Cases and Deaths by Month in the Study districts (2019–2023).

APPENDIX C. MODEL VALIDATION THROUGH PREDICTION OF MALARIA CASES

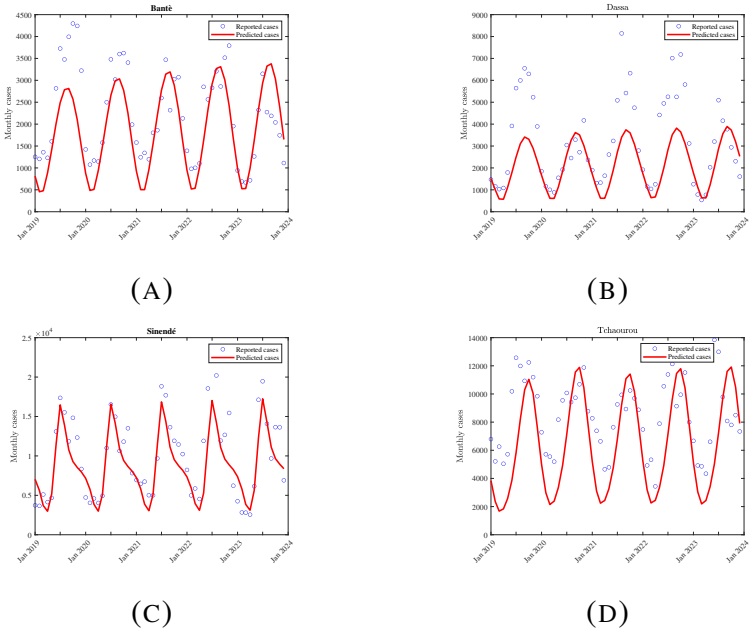

FIGURE 7. Evolution trend of the Malaria monthly cases for each District

APPENDIX D. CONTROL REPRODUCTION NUMBER R_c AGAINST ψ FOR EACH DISTRICT

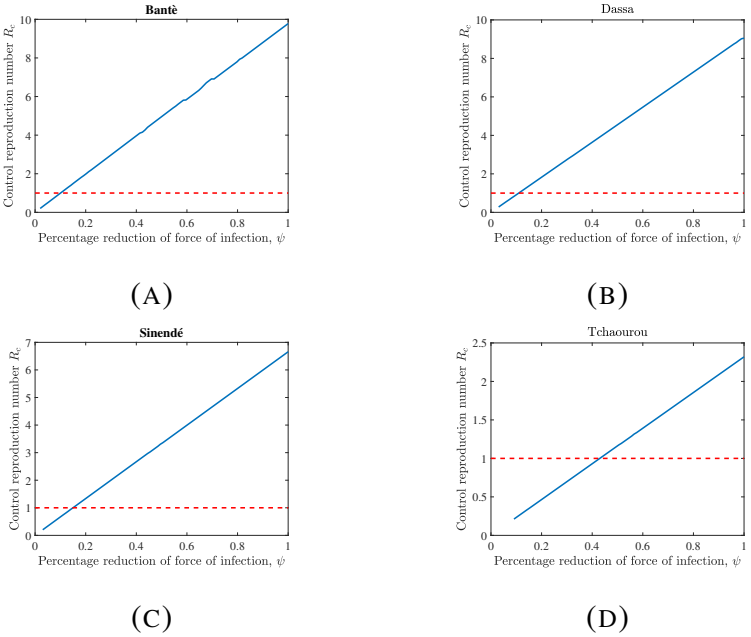

FIGURE 8. Control reproduction number R_c against ψ for each district

APPENDIX E. ALGORITHME TO COMPUTE THE CONTROL REPRODUCTION NUMBER R_c

- For any value of λ, the matrix $W(T,\lambda)$ is determined numerically with MATLAB's `ode45` solver for ordinary differential equations.
- The spectral radius of the matrix $W(T,\lambda)$ is calculated using the Matlab function `max(abs(eig(W(T,lambda))))`.
- Let $h(\lambda) = \rho(W(T,\lambda)) - 1$, the zero of the function h, which represents the control reproduction number R_c, is numerically found using the Matlab function `fzero`.

APPENDIX F. TOTAL POPULATION FOR EACH DISTRICT

TABLE 6. Total population for each district

District	Population
Bantè	131874
Dassa	137954
Sinendé	112792
Tchaourou	274546

ACKNOWLEDGEMENTS

This work was supported by the German Academic Exchange Service– DAAD [grant numbers 57667590 to MLZ- Personal ref.no.: 91871529]. This work was also carried out under the Humboldt Research Hub SEMCA, funded by the German Federal Foreign Office with the support of the Alexander von Humboldt Foundation (AvH). R Glèlè Kakaï acknowledges the Sub-Saharan Africa Advanced Consortium for Biostatistics (SSACAB) Phase II.

CONFLICT OF INTERESTS

The authors declare that there is no conflict of interests.

REFERENCES

[1] World Health Organization, WHO World Malaria Report 2023, (2023). https://www.who.int/teams/global-malaria-programme/reports/world-malaria-report-2023.

[2] S. Bhatt, D.J. Weiss, E. Cameron, D. Bisanzio, B. Mappin, et al., The Effect of Malaria Control on Plasmodium Falciparum in Africa Between 2000 and 2015, Nature 526 (2015), 207–211. https://doi.org/10.1038/nature15535.

[3] World Health Organization, Global technical strategy for malaria 2016-2030, (2015). https://www.who.int/docs/default-source/documents/global-technical-strategy-for-malaria-2016-2030.pdf.

[4] T.A. Tizifa, A.N. Kabaghe, R.S. McCann, H. van den Berg, M. Van Vugt, et al., Prevention Efforts for Malaria, Curr. Trop. Med. Rep. 5 (2018), 41–50. https://doi.org/10.1007/s40475-018-0133-y.

[5] K. Wangdi, L. Furuya-Kanamori, J. Clark, J.J. Barendregt, M.L. Gatton, et al., Comparative Effectiveness of Malaria Prevention Measures: A Systematic Review and Network Meta-Analysis, Parasites Vectors 11 (2018), 210. https://doi.org/10.1186/s13071-018-2783-y.

[6] R.M. Anderson, R.M. May, Infectious Diseases of Humans, Oxford University Press, (1991).

[7] The malERA Consultative Group on Modeling, A Research Agenda for Malaria Eradication: Modeling, PLoS Med. 8 (2011), e1000403. https://doi.org/10.1371/journal.pmed.1000403.

[8] S. Mandal, R.R. Sarkar, S. Sinha, Mathematical Models of Malaria - A Review, Malar. J. 10 (2011), 202. https://doi.org/10.1186/1475-2875-10-202.

[9] L.G. Alvarez-Zuzek, C.E. La Rocca, J.R. Iglesias, L.A. Braunstein, Epidemic Spreading in Multiplex Networks Influenced by Opinion Exchanges on Vaccination, PLOS ONE 12 (2017), e0186492. https://doi.org/10.1371/journal.pone.0186492.

[10] S. Xia, J. Liu, A Computational Approach to Characterizing the Impact of Social Influence on Individuals' Vaccination Decision Making, PLoS ONE 8 (2013), e60373. https://doi.org/10.1371/journal.pone.0060373.

[11] M. Voinson, S. Billiard, A. Alvergne, Beyond Rational Decision-Making: Modelling the Influence of Cognitive Biases on the Dynamics of Vaccination Coverage, PLOS ONE 10 (2015), e0142990. https://doi.org/10.1371/journal.pone.0142990.

[12] R.C. Tyson, S.D. Hamilton, A.S. Lo, B.O. Baumgaertner, S.M. Krone, The Timing and Nature of Behavioural Responses Affect the Course of an Epidemic, Bull. Math. Biol. 82 (2020), 14. https://doi.org/10.1007/s11538-019-00684-z.

[13] S. Funk, M. Salathé, V.A.A. Jansen, Modelling the Influence of Human Behaviour on the Spread of Infectious Diseases: A Review, J. R. Soc. Interface 7 (2010), 1247–1256. https://doi.org/10.1098/rsif.2010.0142.

[14] S. Funk, S. Bansal, C.T. Bauch, K.T. Eames, W.J. Edmunds, et al., Nine Challenges in Incorporating the Dynamics of Behaviour in Infectious Diseases Models, Epidemics 10 (2015), 21–25. https://doi.org/10.1016/j.epidem.2014.09.005.

[15] R. Prieto Curiel, H. González Ramírez, Vaccination Strategies Against COVID-19 and the Diffusion of Anti-Vaccination Views, Sci. Rep. 11 (2021), 6626. https://doi.org/10.1038/s41598-021-85555-1.

[16] M.A. Pires, N. Crokidakis, Dynamics of Epidemic Spreading with Vaccination: Impact of Social Pressure and Engagement, Physica: Stat. Mech. Appl. 467 (2017), 167–179. https://doi.org/10.1016/j.physa.2016.10.004.

[17] M.A. Pires, A.L. Oestereich, N. Crokidakis, Sudden Transitions in Coupled Opinion and Epidemic Dynamics with Vaccination, J. Stat. Mech.: Theory Exp. 2018 (2018), 053407. https://doi.org/10.1088/1742-5468/aabfc6.

[18] R.R. Rapaka, E.A. Hammershaimb, K.M. Neuzil, Are Some COVID-19 Vaccines Better Than Others? Interpreting and Comparing Estimates of Efficacy in Vaccine Trials, Clin. Infect. Dis. 74 (2021), 352–358. https://doi.org/10.1093/cid/ciab213.

[19] R.C. Tyson, N.D. Marshall, B.O. Baumgaertner, Transient Prophylaxis and Multiple Epidemic Waves, AIMS Math. 7 (2022), 5616–5633. https://doi.org/10.3934/math.2022311.

[20] B. She, J. Liu, S. Sundaram, P.E. Pare, On a Networked SIS Epidemic Model with Cooperative and Antagonistic Opinion Dynamics, IEEE Trans. Control. Netw. Syst. 9 (2022), 1154–1165. https://doi.org/10.1109/tcns.2022.3145748.

[21] R. Boucekkine, A. Carvajal, S. Chakraborty, A. Goenka, The Economics of Epidemics and Contagious Diseases: An Introduction, J. Math. Econ. 93 (2021), 102498. https://doi.org/10.1016/j.jmateco.2021.102498.

[22] R.F. Arthur, J.H. Jones, M.H. Bonds, Y. Ram, M.W. Feldman, Adaptive Social Contact Rates Induce Complex Dynamics during Epidemics, PLOS Comput. Biol. 17 (2021), e1008639. https://doi.org/10.1371/journal.pcbi.1008639.

[23] W. Xuan, R. Ren, P.E. Paré, M. Ye, S. Ruf, et al., On a Network SIS Model with Opinion Dynamics, IFAC-PapersOnLine 53 (2020), 2582–2587. https://doi.org/10.1016/j.ifacol.2020.12.305.

[24] B. She, H.C.H. Leung, S. Sundaram, P.E. Pare, Peak Infection Time for a Networked SIR Epidemic with Opinion Dynamics, in: 2021 60th IEEE Conference on Decision and Control (CDC), IEEE, 2021, pp. 2104-2109. https://doi.org/10.1109/cdc45484.2021.9683146.

[25] S. Bhowmick, S. Panja, Influence of Opinion Dynamics to Inhibit Epidemic Spreading Over Multiplex Network, IEEE Control. Syst. Lett. 5 (2021), 1327–1332. https://doi.org/10.1109/lcsys.2020.3035873.

[26] R. Glèlè Kakaï, L.C. Djomatin, An Age-Structured Mathematical Model to Assess the Combined Effects of Vaccine and Non-Vaccine Interventions on Malaria Transmission and Burden, Infect. Dis. Model. 11 (2026), 355–376. https://doi.org/10.1016/j.idm.2025.10.007.

[27] B.O. Baumgaertner, P.A. Fetros, S.M. Krone, R.C. Tyson, Spatial Opinion Dynamics and the Effects of Two Types of Mixing, Phys. Rev. E 98 (2018), 022310. https://doi.org/10.1103/physreve.98.022310.

[28] E. Yedomonhan, C.F. Tovissodé, R.G. Kakaï, Modeling the Effects of Prophylactic Behaviors on the Spread of SARS-Cov-2 in West Africa, Math. Biosci. Eng. 20 (2023), 12955–12989. https://doi.org/10.3934/mbe.2023578.

[29] Johns Hopkins Center for Communication Programs, Enquête sur le Comportement Face au Paludisme: Bénin, 2021, (2022). https://malariabehaviorsurvey.org/wp-content/uploads/2022/11/Benin-MBS-Report-2022-Fr.pdf.

[30] Institut National de la Statistique et de la Démographie (INStaD), Annuaire Etat-Civil 2022, (2022). https://instad.bj/publications/publications-annuelles/593-annuaire-etat-civil-2022.

[31] P. van den Driessche, J. Watmough, Reproduction Numbers and Sub-Threshold Endemic Equilibria for Compartmental Models of Disease Transmission, Math. Biosci. 180 (2002), 29–48. https://doi.org/10.1016/s0025-5564(02)00108-6.

[32] N. Bacaër, S. Guernaoui, The Epidemic Threshold of Vector-Borne Diseases with Seasonality, J. Math. Biol. 53 (2006), 421–436. https://doi.org/10.1007/s00285-006-0015-0.

[33] X. Zhao, Dynamical Systems in Population Biology, Springer, New York, 2003. https://doi.org/10.1007/978-0-387-21761-1.

[34] W. Wang, X. Zhao, Threshold Dynamics for Compartmental Epidemic Models in Periodic Environments, J. Dyn. Differ. Equ. 20 (2008), 699–717. https://doi.org/10.1007/s10884-008-9111-8.

[35] Z. Bai, Y. Zhou, Global Dynamics of an SEIRS Epidemic Model with Periodic Vaccination and Seasonal Contact Rate, Nonlinear Anal.: Real World Appl. 13 (2012), 1060–1068. https://doi.org/10.1016/j.nonrwa.2011.02.008.

[36] M.A. Ibrahim, A. Dénes, Threshold and stability results in a periodic model for malaria transmission with partial immunity in humans, Appl. Math. Comput. 392 (2021), 125711. https://doi.org/10.1016/j.amc.2020.125711

[37] T. Chai, R.R. Draxler, Root Mean Square Error (RMSE) or Mean Absolute Error (MAE)? – Arguments Against Avoiding RMSE in the Literature, Geosci. Model Dev. 7 (2014), 1247–1250. https://doi.org/10.5194/gmd-7-1247-2014.

[38] A. Raue, M. Schilling, J. Bachmann, A. Matteson, M. Schelker, et al., Correction: Lessons Learned from Quantitative Dynamical Modeling in Systems Biology, PLoS ONE 8 (2013), e74335. https://doi.org/10.1371/annotation/ea0193d8-1f7f-492a-b0b7-d877629fdcee.

[39] I. Chou, E.O. Voit, Recent Developments in Parameter Estimation and Structure Identification of Biochemical and Genomic Systems, Math. Biosci. 219 (2009), 57–83. https://doi.org/10.1016/j.mbs.2009.03.002.

[40] The Global Economy, Benin Economic Indicators, (2024). https://www.theglobaleconomy.com/Benin.

[41] N. Chitnis, J.M. Hyman, J.M. Cushing, Determining Important Parameters in the Spread of Malaria Through the Sensitivity Analysis of a Mathematical Model, Bull. Math. Biol. 70 (2008), 1272–1296. https://doi.org/10.1007/s11538-008-9299-0.

[42] W.A. Woldegerima, R. Ouifki, J. Banasiak, Mathematical Analysis of the Impact of Transmission-Blocking Drugs on the Population Dynamics of Malaria, Appl. Math. Comput. 400 (2021), 126005. https://doi.org/10.1016/j.amc.2021.126005.

[43] S. Funk, E. Gilad, C. Watkins, V.A.A. Jansen, The Spread of Awareness and Its Impact on Epidemic Outbreaks, Proc. Natl. Acad. Sci. 106 (2009), 6872–6877. https://doi.org/10.1073/pnas.0810762106.

[44] J.M. Epstein, J. Parker, D. Cummings, R.A. Hammond, Coupled Contagion Dynamics of Fear and Disease: Mathematical and Computational Explorations, PLoS ONE 3 (2008), e3955. https://doi.org/10.1371/journal.pone.0003955.

[45] M.Z. Sadique, W.J. Edmunds, R.D. Smith, W.J. Meerding, O. de Zwart, et al., Precautionary Behavior in Response to Perceived Threat of Pandemic Influenza, Emerg. Infect. Dis. 13 (2007), 1307–1313. https://doi.org/10.3201/eid1309.070372.